J Ginseng Res 43 (2019) 27–37

Contents lists available at ScienceDirect

Journal of Ginseng Research

journal homepage: http://www.ginsengres.org

Research article

Multicomponent assessment and ginsenoside conversions of *Panax quinquefolium* L. roots before and after steaming by HPLC-MS^n

Xin Huang [1], Yan Liu [2,**], Yong Zhang [1], Shuai-Ping Li [1], Hao Yue [1], Chang-Bao Chen [1], Shu-Ying Liu [1,3,*]

[1] Jilin Ginseng Academy, Changchun University of Chinese Medicine, Changchun, China
[2] Institute of Special Animal and Plant Sciences, Chinese Academy of Agricultural Sciences, Changchun, China
[3] Changchun Institute of Applied Chemistry, Chinese Academy of Sciences, Changchun, China

ARTICLE INFO

Article history:
Received 23 March 2017
Received in Revised form
10 July 2017
Accepted 1 August 2017
Available online 5 August 2017

Keywords:
ginsenoside conversions
HPLC-MS^n
multicomponent assessment
Panax quinquefolium L

ABSTRACT

Background: The structural conversions in ginsenosides induced by steaming or heating or acidic condition could improve red ginseng bioactivities significantly. In this paper, the chemical transformations of red American ginseng from fresh *Panax quinquefolium* L. under steaming were investigated, and the possible mechanisms were discussed.
Methods: A method with reversed-phase high-performance liquid chromatography coupled with linear ion trap mass spectrometry (HPLC-MS^n)-equipped electrospray ionization ion source was developed for structural analysis and quantitation of ginsenosides in dried and red American ginseng.
Results: In total, 59 ginsenosides of protopanaxadiol, protopanaxatriol, oleanane, and ocotillol types were identified in American ginseng before and after steaming process by matching the molecular weight and/or comparing MS^n fragmentation with that of standards and/or known published compounds, and some of them were determined to be disappeared or newly generated under different steaming time and temperature. The specific fragments of each aglycone-type ginsenosides were determined as well as aglycone hydrated and dehydrated ones. The mechanisms were deduced as hydrolysis, hydration, dehydration, and isomerization of neutral and acidic ginsenosides. Furthermore, the relative peak areas of detected compounds were calculated based on peak areas ratio.
Conclusion: The multicomponent assessment of American ginseng was conducted by HPLC-MS^n. The result is expected to provide possibility for holistic evaluation of the processing procedures of red American ginseng and a scientific basis for the usage of American ginseng in prescription.

1. Introduction

American ginseng (*Panax quinquefolium* L.) originally grows in southeast of Canada and northern USA, whereas *Panax ginseng* Meyer is commonly referred to ginseng or Korean ginseng. American ginseng and ginseng are of the same Araliaceae and *Panax* genus, present pharmacological activity to reduce stress, enhance immune function and treat several chronic diseases, and so on to improve the quality of life [1–4]. Ginseng has a “warm” property based on the traditional Chinese medicine theory and American ginseng has a “cool” property. Therefore, the efficacy, pharmacological effects, and clinical indications of these two similar roots are different, and they are suitable for different physique and age groups. Ginseng has two types of popular products by drying and steaming process, named white ginseng and red ginseng, respectively. Compared with white ginseng, the red one seemed to show better bioactivity in some cases. Meanwhile, only dried American ginseng is found available in the commercial market.

Ginsenosides are the major pharmacologically active constituents of *Panax* genus. According to the aglycone skeletons, most are the dammarane triterpene type with protopanaxadiol (PPD) and protopanaxatriol (PPT), oleanane type (OLE) and ocotillol type (OCO) of ginsenosides [4,5]. Compared to ginseng, the OCOC-type

* Corresponding author. Jilin Ginseng Academy, Changchun University of Chinese Medicine, Changchun 130117, China.
** Corresponding author. Institute of Special Animal and Plant Sciences, Chinese Academy of Agricultural Sciences, Changchun 130112, China.
E-mail addresses: captainly@gmail.com (Y. Liu), syliu@ciac.jl.cn (S.-Y. Liu).

http://dx.doi.org/10.1016/j.jgr.2017.08.001
p1226-8453 e2093-4947/$ – see front matter

ginsenoside is the characteristic in American ginseng. The ginseng roots also contain ginsenosides with a malonyl or acetyl residue attached to the glucose substituent on C-3 or C-6 position. Ginseng has gained increasing attention in health care; therefore, identification and quantification of the chemical composition of ginseng is necessary for quality, safety, and efficacy control. Many studies of red ginseng have demonstrated that steaming- or heating- or acidic condition-induced ginsenoside structural conversions are significantly related to the biological activities improvement [6–11]. And also some informations on ginsenosides in American ginseng processing were reported [12–14]. Recent studies demonstrated that ginseng presents its efficacy through multi-targeted mechanisms instead of a single chemical constituent influence. Hence, monitoring the chemical components, as many as possible, in red American ginseng processing is important. The structure diversity of ginsenosides are the chemical basis of dried and red American ginseng; they exert different pharmacological activities. During the past few years, many modern techniques have been developed to determine ginsenosides in ginseng. The most commonly used are HPLC-UV [15], HPLC coupled with evaporative light scattering detector [16,17], HPLC combined with electrospray ionization tandem mass spectrometry (HPLC–ESI–MS^n) [18–23], and ultra-performance liquid chromatography/quadrupole time-of-flight MS [24–27]. The ongoing developments of MS permit high sensitivity, selectivity, resolution, and throughput analysis of traditional Chinese medicine. However, the systematic comparison of ginsenosides and chemical transformations between dried and red American ginseng has not been studied and discussed.

In this paper, HPLC-MS^n technique was developed to evaluate the global ginsenosides of dried American ginseng and steaming processed red American ginseng. The 59 main constituents of ginsenosides were identified by combining the complementary fragmentation data for structure confirmation and eluting sequence provided. The relative peak areas of PPD, PPT, OCO, and OLE type components were calculated and compared. Base on the multicomponent assessment approach, the influence of steaming time and temperature on the composition of ginsenosides was determined. The conversions brought about by each type of ginsenosides during steaming process were investigated, and the possible mechanisms were discussed. The validated HPLC-MS^n method demonstrated that holistic chemical profiling as characteristic chemical components to assess the quality of American ginseng and standardize the processing procedures of red American ginseng is reasonable and effective.

2. Materials and methods

2.1. Chemicals and reagents

Methanol (HPLC grade, Fisher Scientific, Waltham, MA), formic acid (HPLC grade, Sigma-Aldrich, Steinheim, Germany), ultrapure water (18 MΩ/cm, Milli-Q water system, Lillipore, Bedford, MA), methanol (analytical grade, Beijing Chemical Works, Beijing, China), and reference ginsenosides Rb_1, Rb_2, Rb_3, Rc, Rd, Re, Rg_1, 20(S)-Rg_2, 20(S)-Rg_3, 20(S)-Rh_1, 20(S)-Rh_2, F_1, F_2, Ro, and 20(R)-pseudoginsenoside F_{11} (Jilin University, Changchun, JL, China) were obtained.

2.2. Reference solution preparation

Reference solutions for 15 ginsenosides were prepared individually by 50% methanol-water to final concentration of 0.1 mg/mL and were diluted with HPLC grade methanol to make desired concentrations for MS^n fragmentation analysis. Each of the individual reference solutions were combined and diluted to obtain final concentrations for HPLC-MS retention time analysis.

2.3. Plant materials and sample preparation

The 5-year-old fresh *Panax quinquefolium* L. roots were collected from Fusong, Jilin province. The botanical origin was identified by Prof Shumin Wang and deposited at the Jilin Ginseng Academy. The main roots with diameter measuring 1–2 cm were chosen for the process experiment (drying and steaming). The dried American ginseng was prepared under sunlight. The red American ginseng was prepared as following: (1) fresh American ginseng roots were cleaned and allowed to air-dry at room temperature; (2) the roots were placed in an autoclave to steam at 100°C or 120°C for 2 h or 4 h or 6 h, separately; (3) the steamed roots were cooled and then dried in a ventilated oven at 50°C for approximately 2–3 d.

Furthermore, 100 g of each root were powdered using a pulverizer and sieved before extraction to assure the analyzed samples were well-distributed and typical. Ultrasonic-assisted extraction of ginsenosides from the pulverized ginseng roots powder (1.0 g) was performed using 80% methanol-water for 30 min. The extraction was repeated thrice with fresh solvent. Then, the extracts were combined, reduced pressure concentrated, and re-dissolved to 1 mL 80% methanol-water. The supernatant was filtered through a 0.45-μm polyvinylidene fluoride syringe filter and used for direct HPLC-MS^n analysis. The extraction of five replicated samples and blank samples was prepared under the same procedure.

2.4. Instrument and condition

HPLC system (Ultimate 3000, Dionex) consists of a quaternary gradient pump, an autosampler, and a thermostatic-column compartment, coupled to linear trap quadrupole (LTQ) linear ion trap mass spectrometer (Thermo Scientific) and controlled with Xcalibur version 3.0 data system software. Thermo Scientific Syncronis C18 HPLC column (100 mm × 2.0 mm, 1.7 μm) was used for separations.

The ESI–MS^n was operated under negative ion mode. The data were acquired in centroid scan mode with normal scan rate and *m/z* 150.0–2000.0 scan range. According to standard calibration procedure, the mass scale was calibrated prior to detection. The sheath gas and aux gas were high purity N_2 with a flow rate of 40 mL/min and 10 mL/min, respectively. The other parameters were set to achieve the best ion signals: electrospray voltage, 3.0 kV; capillary voltage, 20 V; and capillary temperature, 320°C. For the MS^n analyses, the isolation width was 1.0 Da, and collision energies ranged from 10% to 30%. The ginsenoside references were analyzed by infusing individual solutions directly to mass spectrometer at 5 μL/min using the syringe pump.

The mobile phases were 0.1% formic acid in acetonitrile (Solvent A) and 0.1% formic acid in ultrapure water (Solvent B). The gradient elution program with 0.2 mL/min flow rate was as follows: 0–10 min held at 10% A, 10–40 min linearly increased to 100% A, 40–50 min held at 100% A, 50–60 min returned to 10% A. The temperatures of autosampler and column were set at 15°C and 35C°, respectively, and the injection volume was 5 μL.

3. Results and discussion

3.1. Development of HPLC-MS^n method

The LTQ linear ion trap mass spectrometer was applied for determination. First, each ginsenoside solution was analyzed by direct injection in both positive and negative ion modes to check the appropriate ionization mode. The $[M^-H]^-$ ion presented higher

intensity than $[M+H]^+$ ion. Thus, the identification and quantification of ginsenosides were carried out in the negative ion mode by ESI-MS^n and HPLC-MS^n. The spray voltage, capillary temperature, S-lens RF level, and flow rates of sheath gas and aux gas were checked manually to obtain the best experimental conditions. To gain maximum sensitivity and highest signal intensity, the other MS parameters were also optimized by tuning each type of ginsenosides (PPD, PPT, OLE and OCO).

After direct MS analysis, HPLC was coupled to the mass spectrometer via the column cell outlet. After several trials, chromatographic conditions were optimized using American ginseng extraction to ensure the appropriate resolution. The composition of mobile phases considerably affects the transference yield of analytes from liquid to gas in MS detection. Formic acid concentrations (0.1%, 0.05%, and 0.01%) were tested; the best peak shape and improved ionization efficiency lead to a significant signal enhancement. The gradient elution program was investigated to ensure acceptable separation of adjacent peaks.

3.2. *ESI-MS^n and HPLC-ESI-MS analysis of four types of ginsenoside standards*

The structures of four types of ginsenosides (PPD, PPT, OCO, and OLE) are shown in Fig. 1. The aglycones of ginsenosides with dehydration and addition reaction are also presented in Fig. 1. In MS full scan under both positive and negative ion mode, the molecular weights of ginsenosides were easily obtained by their quasi-molecular ions. The characteristic fragmentations of each four types of ginsenoside standards were investigated and summarized in Table 1. According to the specific fragments of each type of ginsenosides, the substituted saccharide chain types and sequence and the aglycone type were determined. The nomenclature for ginsenoside fragmentation is based on the description given by Domon and Costello [28] and Liu et al. [29]. The saccharide substitution at C-20 is α chain, while saccharide substitution at C-3 (PPD) or C-6 (PPT) is β chain [29]. Ions (produced by glycoside cleavages) retaining the charge at the reducing terminus are termed Y and Z, whereas product ions retaining the charge at the non-reducing terminus are termed B and C [28,29]. Cross-ring cleavages produced ions retaining the charge at the reducing terminus are termed X, and product ions retaining the charge at the non-reducing terminus are termed A, with superscript numbers indicating the two bonds cleavage [28,29]. Take Rb_1 and Re as an example, the fragmentation nomenclature of PPD- and PPT-type ginsenosides are shown in Scheme 1.

For PPD-type ginsenoside Rb_1, the $Y_{1\alpha}$ ion at *m/z* 945 is generated by loss of a glucose residue (162 Da). And the $C_{1\alpha}$ ion at *m/z* 179 is also demonstrated that the terminal residue in an α saccharide chain at C-20 of Rb_1 is glucose residue. The $Y_{0\alpha}$ ion at *m/z* 783 is corresponding to the loss of glucose-glucose residue (162 Da + 162 Da). And the $B_{2\alpha}$ ion at *m/z* 323 provides further information for glucose-glucose linkage. The $Y'_{1\beta}$ ion at *m/z* 621 is produced by the loss of glucose-glucose residue (162 Da + 162 Da) at α saccharide chain and glucose residue (162 Da) at β saccharide chain. The $Y'_{0\beta}$ ion at *m/z* 459 is generated by the loss of glucose-glucose residue (162 Da + 162 Da) at α saccharide chain and glucose-glucose residue (162 Da + 162 Da) at β saccharide chain. The *m/z* 101 ($^{2,5}A_{1\alpha}/^{2,5}A_{1\beta}$) ion and *m/z* 221 ($^{0,4}A_{2\alpha}/^{1,3}A_{2\beta}$) ion are corresponding to the cross-ring cleavage products of glucose and glucose-glucose terminals at α or β saccharide chains. According to the other

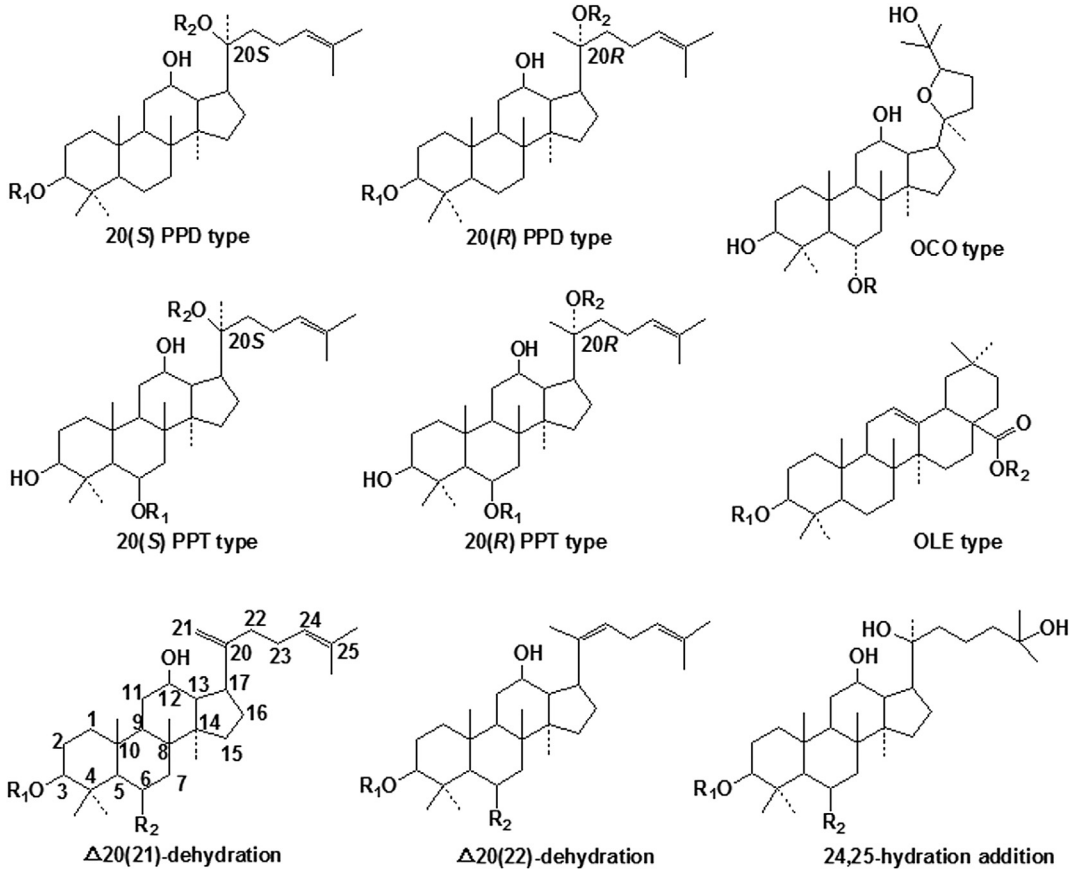

Fig. 1. The aglycone structures of protopanaxadiol, protopanaxatriol, oleanane, and ocotillol types of ginsenosides and their dehydration and hydration addition ginsenosides. OCO, ocotillol; OLE, oleanane; PPD, protopanaxadiol; PPT, protopanaxatriol.

Table 1
The ginsenosides identified in dried and red American ginseng. Ac, acetyl; Mal, malonyl

t_R	Compounds	Molecular formula	Molecular mass	$[M-H]^-$	MS^n fragments
19.31	20(S)-Rf_2	$C_{42}H_{74}O_{14}$	802.5	801.7	619($Y_{1\beta}$), 145($B_{1\beta}$), 493($Y_{0\beta}$), 307($B_{2\beta}$), 101($^{0,2}A_{1\beta}$), 205($^{1,3}A_{2\beta}$), 279($^{1,5}A_{2\beta}$)
19.95	20(R)-Rf_2	$C_{42}H_{74}O_{14}$	802.5	801.7	619($Y_{1\beta}$), 145($B_{1\beta}$), 493($Y_{0\beta}$), 307($B_{2\beta}$), 101($^{0,2}A_{1\beta}$), 205($^{1,3}A_{2\beta}$), 279($^{1,5}A_{2\beta}$)
21.20	Re	$C_{48}H_{82}O_{18}$	946.6	945.7	783($Y_{0\alpha}$), 179($C_{1\alpha}$), 637($Y'_{1\beta}$), 145($B_{1\beta}$), 475($Y'_{0\beta}$), 307($B_{2\beta}$), 101($^{2,5}A_{1\alpha}/^{0,2}A_{1\beta}$), 205($^{1,3}A_{2\beta}$), 279($^{1,5}A_{2\beta}$)
21.22	Rg_1	$C_{42}H_{72}O_{14}$	800.5	799.8	637($Y_{0\alpha}$), 179($C_{1\alpha}$), 475($Y'_{0\beta}$), 161($B_{1\beta}$), 101($^{2,5}A_{1\alpha}/^{2,5}A_{1\beta}$)
22.56	Malonyl-Rg_1	$C_{45}H_{74}O_{17}$	886.5	885.6	799[M-H-Mal]$^-$, 637($Y_{0\alpha}$), 179($C_{1\alpha}$), 475($Y'_{0\beta}$), 161($B_{1\beta}$), 101($^{2,5}A_{1\alpha}/^{2,5}A_{1\beta}$)
22.76	24(S)-Pseudo-F_{11}	$C_{42}H_{72}O_{14}$	800.5	799.8	653($Y_{1\beta}$), 145($B_{1\beta}$), 491($Y_{0\beta}$), 307($B_{2\beta}$), 101($^{0,2}A_{1\beta}$), 205($^{1,3}A_{2\beta}$), 279($^{1,5}A_{2\beta}$)
24.28	Compound Mc	$C_{42}H_{72}O_{11}$	752.5	751.5	621($Y_{1\alpha}$), 145($C_{1\alpha}$), 459($Y_{0\alpha}$), 293($B_{2\alpha}$), 191($^{0,4}A_{2\alpha}$)
26.45	Acetyl-Rg_1	$C_{44}H_{74}O_{15}$	842.5	841.6	799[M-H-Ac]$^-$, 637($Y_{0\alpha}$), 179($C_{1\alpha}$), 475($Y'_{0\beta}$), 161($B_{1\beta}$), 101($^{2,5}A_{1\alpha}/^{2,5}A_{1\beta}$)
26.95	Pseudo-RT_2	$C_{41}H_{70}O_{14}$	786.5	785.6	653($Y_{1\beta}$), 131($B_{1\beta}$), 491($Y_{0\beta}$), 293($B_{2\beta}$), 191($^{1,3}A_{2\beta}$), 265($^{1,5}A_{2\beta}$)
27.29	24(R)-Pseudo-F_{11}	$C_{42}H_{72}O_{14}$	800.5	799.8	653($Y_{1\beta}$), 145($B_{1\beta}$), 491($Y_{0\beta}$), 307($B_{2\beta}$), 101($^{0,2}A_{1\beta}$), 205($^{1,3}A_{2\beta}$), 279($^{1,5}A_{2\beta}$)
27.77	Pseudo-RT_5	$C_{36}H_{62}O_{10}$	654.4	653.8	491($Y_{0\beta}$), 161($B_{1\beta}$), 101($^{2,5}A_{1\beta}$)
28.55	Rb_1	$C_{54}H_{92}O_{23}$	1108.6	1107.8	945($Y_{1\alpha}$), 179($C_{1\alpha}$), 783($Y_{0\alpha}$), 323($B_{2\alpha}$), 621($Y'_{1\beta}$), 459($Y'_{0\beta}$), 101($^{2,5}A_{1\alpha}/^{2,5}A_{1\beta}$), 221($^{0,4}A_{2\alpha}/^{1,3}A_{2\beta}$)
28.57	Pseudo-F_8	$C_{55}H_{92}O_{23}$	1120.6	1119.8	1077[M-H-Ac]$^-$, 945($Y_{1\alpha}$), 149($C_{1\alpha}$), 783($Y_{0\alpha}$), 293($B_{2\alpha}$), 621($Y'_{1\beta}$), 459($Y'_{0\beta}$), 191($^{0,4}A_{2\alpha}$), 101($^{2,5}A_{1\beta}$), 221($^{1,3}A_{2\beta}$)
29.02	Malonyl-Rb_1	$C_{57}H_{94}O_{26}$	1194.6	1193.8	1107[M-H-Mal]$^-$, 945($Y_{1\alpha}$), 179($C_{1\alpha}$), 783($Y_{0\alpha}$), 323($B_{2\alpha}$), 621($Y'_{1\beta}$), 459($Y'_{0\beta}$), 101($^{2,5}A_{1\alpha}/^{2,5}A_{1\beta}$), 191($^{0,4}A_{2\alpha}$), 221($^{1,3}A_{2\beta}$)
29.21	20(S)-Rg_2	$C_{42}H_{72}O_{13}$	784.5	783.8	637($Y_{1\beta}$), 145($B_{1\beta}$), 475($Y_{0\beta}$), 307($B_{2\beta}$), 101($^{0,2}A_{1\beta}$), 205($^{1,3}A_{2\beta}$), 279($^{1,5}A_{2\beta}$)
29.48	Rc	$C_{53}H_{90}O_{22}$	1078.6	1077.7	945($Y_{1\alpha}$), 149($C_{1\alpha}$), 783($Y_{0\alpha}$), 293($B_{2\alpha}$), 621($Y'_{1\beta}$), 459($Y'_{0\beta}$), 191($^{0,4}A_{2\alpha}$), 101($^{2,5}A_{1\beta}$), 221($^{1,3}A_{2\beta}$)
29.56	20(R)-Rg_2	$C_{42}H_{72}O_{13}$	784.5	783.8	637($Y_{1\beta}$), 145($B_{1\beta}$), 475($Y_{0\beta}$), 307($B_{2\beta}$), 101($^{0,2}A_{1\beta}$), 205($^{1,3}A_{2\beta}$), 279($^{1,5}A_{2\beta}$)
29.71	20(S)-Rh_1	$C_{36}H_{62}O_9$	638.4	637.9	475($Y_{0\beta}$), 161($B_{1\beta}$), 101($^{2,5}A_{1\beta}$)
29.88	Ro	$C_{48}H_{76}O_{19}$	956.5	955.9	793($Y_{0\alpha}$/$Y_{1\beta}$), 631($Y'_{1\beta}$), 455($Y'_{0\beta}$), 101($^{2,5}A_{1\alpha}/^{2,5}A_{1\beta}$), 119($^{0,2}A_{1\beta}$), 221($^{1,3}A_{2\beta}$)
29.97	Malonyl-Rc	$C_{56}H_{92}O_{25}$	1164.6	1163.7	1077[M-H-Mal]$^-$, 945($Y_{1\alpha}$), 149($C_{1\alpha}$), 783($Y_{0\alpha}$), 293($B_{2\alpha}$), 621($Y'_{1\beta}$), 459($Y'_{0\beta}$), 191($^{0,4}A_{2\alpha}$), 101($^{2,5}A_{1\beta}$), 221($^{1,3}A_{2\beta}$)
30.30	Rb_2	$C_{53}H_{90}O_{22}$	1078.6	1077.6	945($Y_{1\alpha}$), 149($C_{1\alpha}$), 783($Y_{0\alpha}$), 293($B_{2\alpha}$), 621($Y'_{1\beta}$), 459($Y'_{0\beta}$), 191($^{0,4}A_{2\alpha}$), 101($^{2,5}A_{1\beta}$), 221($^{1,3}A_{2\beta}$)
30.40	20(R)-Rh_1	$C_{36}H_{62}O_9$	638.4	637.8	475($Y_{0\beta}$), 161($B_{1\beta}$), 101($^{2,5}A_{1\beta}$)
30.53	Rb_3	$C_{53}H_{90}O_{22}$	1078.6	1077.7	945($Y_{1\alpha}$), 149($C_{1\alpha}$), 783($Y_{0\alpha}$), 293($B_{2\alpha}$), 621($Y'_{1\beta}$), 459($Y'_{0\beta}$), 191($^{0,4}A_{2\alpha}$), 101($^{2,5}A_{1\beta}$), 221($^{1,3}A_{2\beta}$)
30.72	Malonyl-Rb_2	$C_{56}H_{92}O_{25}$	1164.6	1163.6	1077[M-H-Mal]$^-$, 945($Y_{1\alpha}$), 149($C_{1\alpha}$), 783($Y_{0\alpha}$), 293($B_{2\alpha}$), 621($Y'_{1\beta}$), 459($Y'_{0\beta}$), 191($^{0,4}A_{2\alpha}$), 101($^{2,5}A_{1\beta}$), 221($^{1,3}A_{2\beta}$)
30.95	Malonyl-Rb_3	$C_{56}H_{92}O_{25}$	1164.0	1163.6	1077[M-H-Mal]$^-$, 945($Y_{1\alpha}$), 149($C_{1\alpha}$), 783($Y_{0\alpha}$), 293($B_{2\alpha}$), 621($Y'_{1\beta}$), 459($Y'_{0\beta}$), 191($^{0,4}A_{2\alpha}$), 101($^{2,5}A_{1\beta}$), 221($^{1,3}A_{2\beta}$)
31.22	Quinquefolium R_1	$C_{56}H_{94}O_{24}$	1150.5	1149.7	1107[M-H-Ac]$^-$, 945($Y_{1\alpha}$), 179($C_{1\alpha}$), 783($Y_{0\alpha}$), 323($B_{2\alpha}$), 621($Y'_{1\beta}$), 459($Y'_{0\beta}$), 101($^{2,5}A_{1\alpha}/^{2,5}A_{1\beta}$), 191($^{0,4}A_{2\alpha}$), 221($^{1,3}A_{2\beta}$)
31.52	24(R)-Vina-R_1	$C_{44}H_{74}O_{15}$	842.5	841.6	799[M-H-Ac]$^-$, 653($Y_{1\beta}$), 145($B_{1\beta}$), 491($Y_{0\beta}$), 307($B_{2\beta}$), 101($^{0,2}A_{1\beta}$), 205($^{1,3}A_{2\beta}$), 279($^{1,5}A_{2\beta}$)
31.61	Pseudo-RT_1	$C_{47}H_{74}O_{18}$	926.5	925.8	763($Y_{0\alpha}$), 793($Y_{1\beta}$), 631($Y'_{1\beta}$), 455($Y'_{0\beta}$), 101($^{2,5}A_{1\alpha}$), 105($^{0,2}A_{1\beta}$), 191($^{1,3}A_{2\beta}$)
32.02	F_1	$C_{36}H_{62}O_9$	638.4	637.8	475($Y_{0\alpha}$), 179($C_{1\alpha}$), 101($^{2,5}A_{1\alpha}$)
32.12	Quinquefolium I	$C_{52}H_{86}O_{19}$	1014.6	1013.7	945[M-H-68]$^-$, 783($Y_{0\alpha}$), 161($B_{1\alpha}$), 621($Y'_{1\beta}$), 459($Y'_{0\beta}$), 101($^{2,5}A_{1\alpha}/^{2,5}A_{1\beta}$), 221($^{1,3}A_{2\beta}$)
32.13	Rd	$C_{48}H_{82}O_{18}$	946.6	945.9	783($Y_{0\alpha}$), 161($B_{1\alpha}$), 621($Y'_{1\beta}$), 459($Y'_{0\beta}$), 101($^{2,5}A_{1\alpha}/^{2,5}A_{1\beta}$), 221($^{1,3}A_{2\beta}$)
32.45	Malonyl-Rd	$C_{51}H_{84}O_{21}$	1032.6	1031. 7	945[M-H-Mal]$^-$, 783($Y_{0\alpha}$), 161($B_{1\alpha}$), 621($Y'_{1\beta}$), 459($Y'_{0\beta}$), 101($^{2,5}A_{1\alpha}/^{2,5}A_{1\beta}$), 221($^{1,3}A_{2\beta}$)
32.57	Chikusetsusaponin IVa	$C_{42}H_{66}O_{14}$	794.5	793.9	631($Y_{0\alpha}$), 455($Y'_{0\beta}$), 101($^{2,5}A_{1\alpha}$), 149($^{0,2}A_{1\beta}$)
32.66	Rs_1	$C_{55}H_{92}O_{23}$	1120.6	1119.3	1077[M-H-Ac]$^-$, 945($Y_{1\alpha}$), 149($C_{1\alpha}$), 783($Y_{0\alpha}$), 293($B_{2\alpha}$), 621($Y'_{1\beta}$), 459($Y'_{0\beta}$), 191($^{0,4}A_{2\alpha}$), 101($^{2,5}A_{1\beta}$), 221($^{1,3}A_{2\beta}$)
32.81	Rs_2	$C_{55}H_{92}O_{23}$	1120.6	1119.6	1077[M-H-Ac]$^-$, 945($Y_{1\alpha}$), 149($C_{1\alpha}$), 783($Y_{0\alpha}$), 293($B_{2\alpha}$), 621($Y'_{1\beta}$), 459($Y'_{0\beta}$), 191($^{0,4}A_{2\alpha}$), 101($^{2,5}A_{1\beta}$), 221($^{1,3}A_{2\beta}$)
33.09	20(S)-acetyl-Rg_2	$C_{44}H_{74}O_{14}$	826.5	825.7	783[M-H-Ac]$^-$, 637($Y_{1\beta}$), 145($B_{1\beta}$), 475($Y_{0\beta}$), 307($B_{2\beta}$), 101($^{0,2}A_{1\beta}$), 205($^{1,3}A_{2\beta}$), 279($^{1,5}A_{2\beta}$)
33.29	Gypenoside X VII	$C_{48}H_{82}O_{18}$	946.6	945.7	783($Y_{1\alpha}$), 179($C_{1\alpha}$), 621($Y_{0\alpha}$), 323($B_{2\alpha}$), 459($Y'_{0\beta}$), 101($^{2,5}A_{1\alpha}/^{2,5}A_{1\beta}$), 221($^{0,4}A_{2\alpha}$)
33.30	20(R)-acetyl-Rg_2	$C_{44}H_{74}O_{14}$	826.5	825.7	783[M-H-Ac]$^-$, 637($Y_{1\beta}$), 145($B_{1\beta}$), 475($Y_{0\beta}$), 307($B_{2\beta}$), 101($^{0,2}A_{1\beta}$), 205($^{1,3}A_{2\beta}$), 279($^{1,5}A_{2\beta}$)
33.99	Pseudo-RC_1	$C_{50}H_{84}O_{19}$	988.6	987.8	945[M-H-Ac]$^-$, 783($Y_{0\alpha}$), 161($B_{1\alpha}$), 621($Y'_{1\beta}$), 459($Y'_{0\beta}$), 101($^{2,5}A_{1\alpha}/^{2,5}A_{1\beta}$), 221($^{1,3}A_{2\beta}$)
34.64	Quinquefolium III	$C_{50}H_{84}O_{19}$	988.6	987.7	945[M-H-Ac]$^-$, 783($Y_{0\alpha}$), 161($B_{1\alpha}$), 621($Y'_{1\beta}$), 459($Y'_{0\beta}$), 101($^{2,5}A_{1\alpha}/^{2,5}A_{1\beta}$), 221($^{1,3}A_{2\beta}$)
35.11	Rg_6	$C_{42}H_{70}O_{12}$	766.5	765.9	619($Y_{1\beta}$), 145($B_{1\beta}$), 457($Y_{0\beta}$), 307($B_{2\beta}$), 101($^{0,2}A_{1\beta}$), 205($^{1,3}A_{2\beta}$), 279($^{1,5}A_{2\beta}$)
35.44	Rg_4	$C_{42}H_{70}O_{12}$	766.5	765.8	619($Y_{1\beta}$), 145($B_{1\beta}$), 457($Y_{0\beta}$), 307($B_{2\beta}$), 101($^{0,2}A_{1\beta}$), 205($^{1,3}A_{2\beta}$), 279($^{1,5}A_{2\beta}$)
35.69	F_2	$C_{42}H_{72}O_{13}$	784.5	783.5	621($Y_{0\alpha}$), 161($B_{1\alpha}$), 459($Y'_{0\beta}$), 101($^{2,5}A_{1\alpha}$)
35.96	Rk_3	$C_{36}H_{60}O_8$	620.4	619.9	457($Y_{0\beta}$), 161($B_{1\beta}$), 101($^{2,5}A_{1\beta}$)
36.05	Zingibroside R_1	$C_{42}H_{66}O_{14}$	794.5	793.9	631($Y_{1\beta}$), 455($Y_{0\beta}$), 101($^{2,5}A_{1\beta}$), 221($^{1,3}A_{2\beta}$)
36.37	Rh_4	$C_{36}H_{60}O_8$	620.4	619.9	457($Y_{0\beta}$), 161($B_{1\beta}$), 101($^{2,5}A_{1\beta}$)
36.81	20(S)-Rg_3	$C_{42}H_{72}O_{13}$	784.5	783.8	621($Y_{1\beta}$), 179($C_{1\beta}$), 459($Y_{0\beta}$), 323($B_{2\beta}$), 101($^{2,5}A_{1\beta}$), 221($^{1,3}A_{2\beta}$)
37.01	20(R)-Rg_3	$C_{42}H_{72}O_{13}$	784.5	783.8	621($Y_{1\beta}$), 179($C_{1\beta}$), 459($Y_{0\beta}$), 323($B_{2\beta}$), 101($^{2,5}A_{1\beta}$), 221($^{1,3}A_{2\beta}$)
38.62	20(S)-Rs_3	$C_{44}H_{74}O_{14}$	826.5	825.9	783[M-H-Ac]$^-$, 621($Y_{1\beta}$), 179($C_{1\beta}$), 459($Y_{0\beta}$), 323($B_{2\beta}$), 101($^{2,5}A_{1\beta}$), 221($^{1,3}A_{2\beta}$)
38.78	Calenduloside E	$C_{36}H_{56}O_9$	632.4	631.8	455($Y_{0\beta}$), 149($^{0,2}A_{1\beta}$)
38.85	20(R)-Rs_3	$C_{44}H_{74}O_{14}$	826.5	825.9	783[M-H-Ac]$^-$, 621($Y_{1\beta}$), 179($C_{1\beta}$), 459($Y_{0\beta}$), 323($B_{2\beta}$), 101($^{2,5}A_{1\beta}$), 221($^{1,3}A_{2\beta}$)
39.72	Rk_1	$C_{42}H_{70}O_{12}$	766.5	765.5	603($Y_{1\beta}$), 161($B_{1\beta}$), 441($Y_{0\beta}$), 323($B_{2\beta}$), 101($^{2,5}A_{1\beta}$), 221($^{1,3}A_{2\beta}$)
40.04	Rg_5	$C_{42}H_{70}O_{12}$	766.5	765.5	603($Y_{1\beta}$), 161($B_{1\beta}$), 441($Y_{0\beta}$), 323($B_{2\beta}$), 101($^{2,5}A_{1\beta}$), 221($^{1,3}A_{2\beta}$)
41.16	20(S)-Rh_2	$C_{36}H_{62}O_8$	622.4	621.7	459($Y_{0\beta}$), 161($B_{1\beta}$), 101($^{2,5}A_{1\beta}$)
41.42	20(R)-Rh_2	$C_{36}H_{62}O_8$	622.4	621.7	459($Y_{0\beta}$), 161($B_{1\beta}$), 101($^{2,5}A_{1\beta}$)
41.77	Rs_5	$C_{44}H_{72}O_{13}$	808.5	807.6	765[M-H-Ac]$^-$, 603($Y_{1\beta}$), 161($B_{1\beta}$), 441($Y_{0\beta}$), 323($B_{2\beta}$), 101($^{2,5}A_{1\beta}$), 221($^{1,3}A_{2\beta}$)
42.08	Rs_4	$C_{44}H_{72}O_{13}$	808.5	807.6	765[M-H-Ac]$^-$, 603($Y_{1\beta}$), 161($B_{1\beta}$), 441($Y_{0\beta}$), 323($B_{2\beta}$), 101($^{2,5}A_{1\beta}$), 221($^{1,3}A_{2\beta}$)
46.25	Rk_2	$C_{36}H_{60}O_7$	604.5	603.4	441($Y_{0\beta}$), 161($B_{1\beta}$), 101($^{2,5}A_{1\beta}$)
46.52	Rh_3	$C_{36}H_{60}O_7$	604.5	603.4	441($Y_{0\beta}$), 161($B_{1\beta}$), 101($^{2,5}A_{1\beta}$)

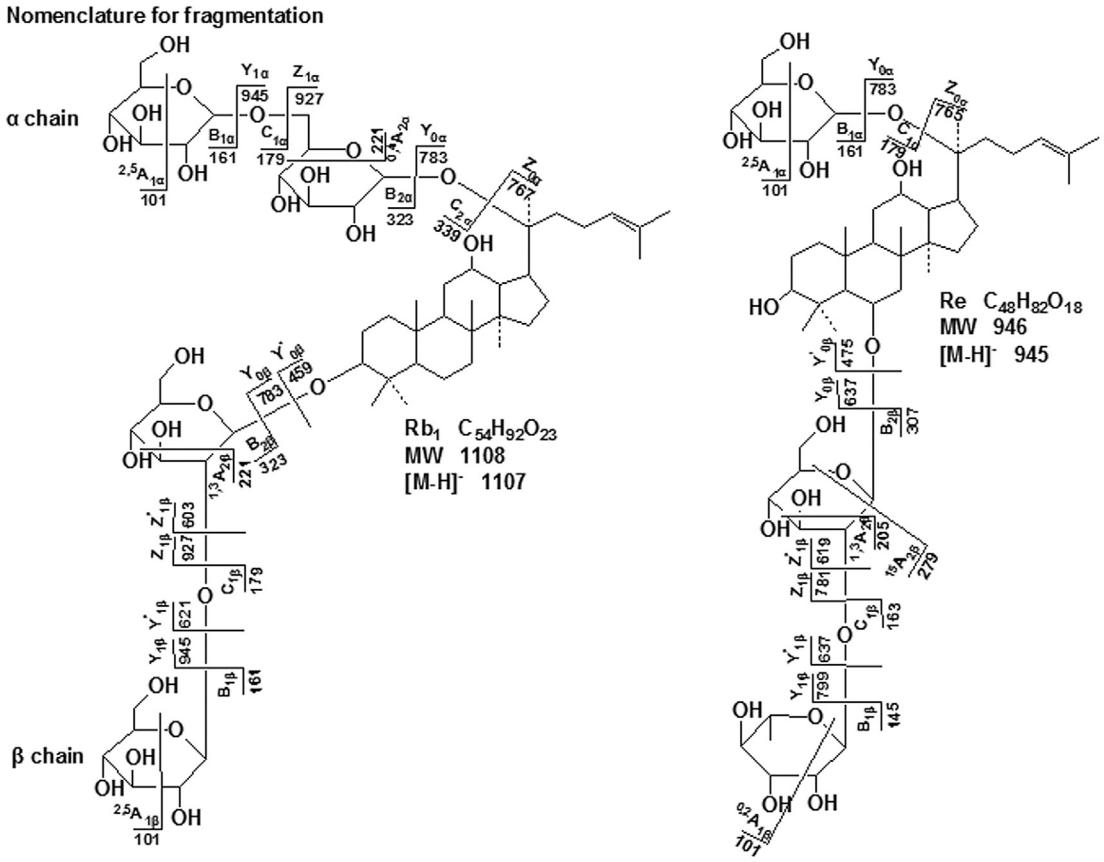

Scheme 1. The fragmentation nomenclature of protopanaxadiol and protopanaxatriol types of ginsenosides Rb_1 and Re.

authentic PPD-type ginsenoside standards (Rb_2, Rb_3, Rc, Rd, 20(S)-Rg_3, 20(S)-Rh_2, F_2) fragmentation pathway, the *m/z* 459 ion is the typical aglycone of PPD-type ginsenosides. The specific neutral monosaccharide residue losses are 162 Da, 146 Da, and 132 Da corresponding to glucose, rhamnose, and arabinose or xylose substitutions, respectively.

For PPT-type ginsenoside Re, the $Y_{0\alpha}$ ion at *m/z* 783 is generated by the loss of a glucose residue (162 Da). And the $C_{1\alpha}$ ion at *m/z* 179 is also demonstrated that the terminal residue in an α saccharide chain at C-20 of Re is glucose residue. The $Y'_{1\beta}$ ion at *m/z* 637 is produced by the loss of glucose residue (162 Da) at α saccharide chain and rhamnose residue (146 Da) at β saccharide chain. And the $B_{1\beta}$ ion at *m/z* 145 provides further information for rhamnose residue at β saccharide r chain. The $Y'_{0\beta}$ ion at *m/z* 475 is generated by the loss of glucose residue (162 Da) at α saccharide chain and rhamnose-glucose residue (146 Da + 162 Da) at β saccharide chain. And the $B_{2\beta}$ ion at *m/z* 307 also provides further information for rhamnose-glucose residue at β saccharide chain. The *m/z* 101 ($^{2,5}A_{1\alpha}/^{0,2}A_{1\beta}$) ion, *m/z* 205 ($^{1,3}A_{2\beta}$) ion, and *m/z* 279 ($^{1,5}A_{2\beta}$) ion are corresponding to the cross-ring cleavage products of glucose and rhamnose-glucose terminals at α or β saccharide chains. According to the other authentic PPT-type ginsenoside standards (Rg_1, 20(S)-Rg_2, 20(S)-Rh_1, F_1) fragmentation pathway, the *m/z* 475 ion is the characteristic aglycone of PPT-type ginsenosides. The specific neutral saccharide residue losses are 162 Da, 132 Da, and 146 Da corresponding to glucose, rhamnose, and arabinose or xylose substitutions, respectively.

For OCO-type pseudoginsenoside F_{11}, the $Y_{1\beta}$ ion at *m/z* 653 is produced by the loss of rhamnose residue (146 Da) at β saccharide chain. And the $B_{1\beta}$ ion at *m/z* 145 provides further information for rhamnose residue at β saccharide chain. The $Y_{0\beta}$ ion at *m/z* 491 is generated by the loss of rhamnose-glucose residue (146 Da + 162 Da) at β saccharide chain; it is the characteristic aglycone of OCO type ginsenosides. And the $B_{2\beta}$ ion at *m/z* 307 also provides further information for rhamnose-glucose residue at β saccharide chain. The *m/z* 101 ($^{0,2}A_{1\beta}$) ion, *m/z* 205 ($^{1,3}A_{2\beta}$) ion, and *m/z* 279 ($^{1,5}A_{2\beta}$) ion are corresponding to the cross-ring cleavage products of glucose and rhamnose-glucose terminals at β saccharide chain.

For the OLE-type ginsenoside Ro, the fragment ion at *m/z* 793 ($Y_{0\alpha}/Y_{1\beta}$) is generated by the loss of a glucose residue (162 Da) in α or β saccharide chain. The $Y'_{1\beta}$ ion at *m/z* 631 is produced by the loss of glucose residue (162 Da) at α saccharide chain and glucose residue (162 Da) at β saccharide chain. The $Y'_{0\beta}$ ion at *m/z* 455 is produced by losing glucose residue (162 Da) at α saccharide chain and glucose-glucose residue (162 Da + 162 Da) at β saccharide chain; it is the characteristic aglycone of OLE-type ginsenosides. The *m/z* 101 ($^{2,5}A_{1\alpha}/^{2,5}A_{1\beta}$) ion, *m/z* 119 ($^{0,2}A_{1\beta}$) ion and *m/z* 221 ($^{1,3}A_{2\beta}$) ion are corresponding to the cross-ring cleavage products of glucose and glucose-glucose terminals at α or β saccharide chains.

Composite 15 ginsenosides standards were analyzed by HPLC-ESI-MS for retention time determination. The molecular weights, fragmentation patterns, and retention times were useful for identification of ginsenoside structures in complex mixtures.

3.3. Ginsenoside profiling of dried and red American ginseng

The ginsenoside profiling of dried and red American ginseng extracts were analyzed by HPLC-ESI-MS^n to determine the retention time, molecular weight information, aglycone type, and saccharide substitution sequences according to characteristic fragmentation. Fig. 2 showed the HPLC-MS total ion chromatogram (TIC) in the negative ion mode of the ginsenosides of dried

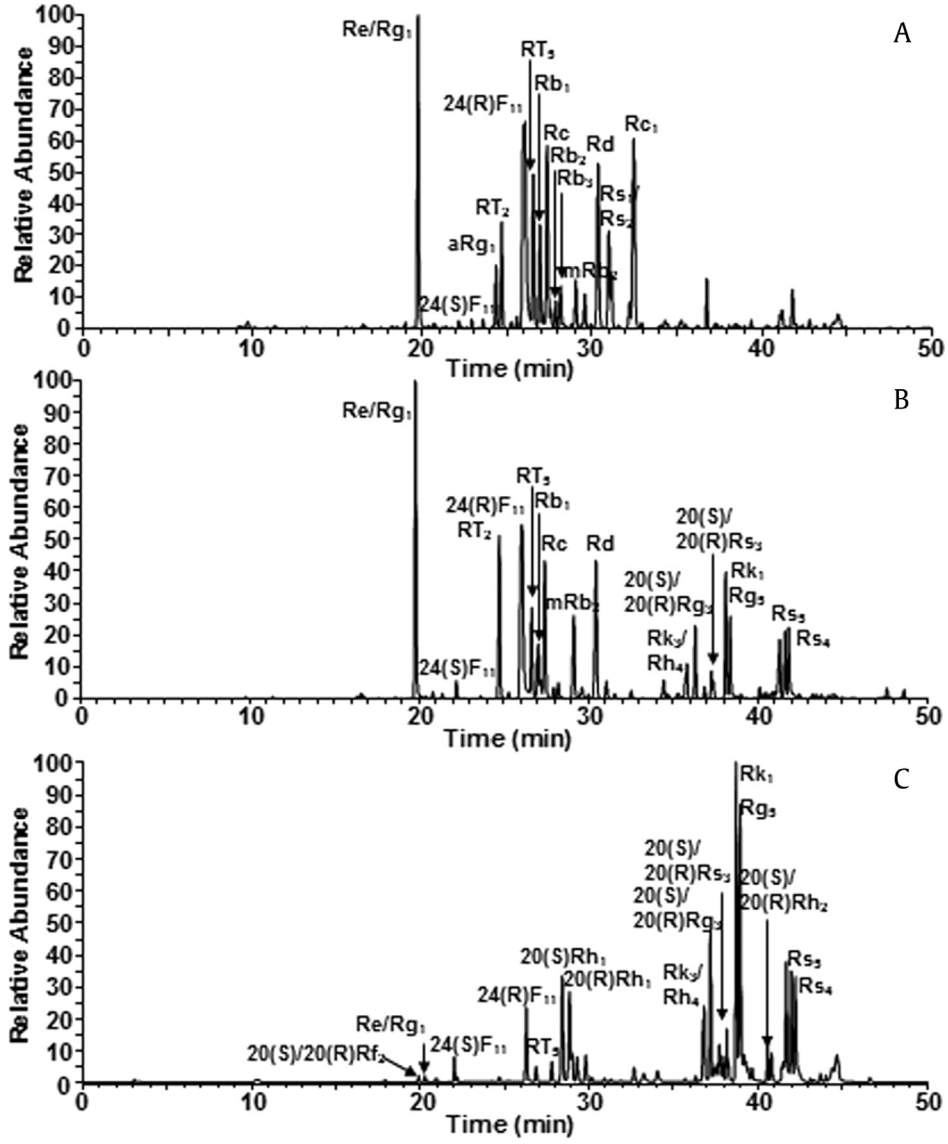

Fig. 2. The HPLC-MS total ion chromatogram of the ginsenosides extracts of (A) dried American Ginseng; (B) red American Ginseng (100°C for 2 h); and (C) red American Ginseng (120°C for 6 h) in the negative ion mode.

and red American Ginseng (100°C and 120°C) extracts. Approximately 59 major ginsenosides were investigated, 15 of which were unambiguous identified by comparison of retention times, molecular weight, and specific fragmentations with standards. The other peaks of TIC were tentatively identified by matching the molecular weight with the reported information of known ginsenosides and further verified by characteristic fragment pathways to provide structural information for the elucidation of results. The detailed identifications of components are listed in Table 1. As the ginsenosides presented similar polarity and isomerization, the appropriate chromatographic gradient and extracted ion chromatogram were applied to analyze the overlapped and isomeric peaks.

The observation of *m/z* 459 fragment ion provided evidence of PPD-type aglycone ginsenosides' presence. Within this group, $[M-H]^-$ ion at *m/z* 1107 (Rb_1), 1077 (Rb_2, Rb_3, Rc), 945 (Rd), 783 (20(S)-Rg_3, F_2), 621 (20(S)-Rh_2) were identified by comparison with retention time and specific fragment ions of ginsenoside references. Due to the unavailability of 20(R) epimer references, 20(R)-Rg_3 and 20(R)-Rh_2 were distinguished with their 20(S) epimers on the basis of their chromatographic behavior, as the 20(S) epimer was reported to elute earlier than its 20(R) epimer. Malonylated and acetylated ginsenosides were detected as characteristic fragments $[M\text{-malonyl}]^-$ or $[M\text{-acetyl}]^-$ by the loss of 86 Da or 42 Da in MS^2. And in MS^n experiment, the observed fragment ions accorded with their corresponding neutral ginsenosides. Some peaks showed PPD-type aglycone with dehydration at *m/z* 441, which is △20(21)- or △20(22)-dehydrated-PPD specific ion. And △20(21)-isomers were reported to elute earlier than its △20(22)-isomers. Therefore, peaks at *m/z* 765 (Rk_1, Rg_5) and 603 (Rk_2, Rh_3) were identified.

For the peaks presented, *m/z* 475 fragment ions were classified as PPT-type ginsenosides, as shown in Table 1. The specific ion at *m/z* 493 and 457 yielded from PPT aglycone ion (*m/z* 475) with +18 Da and −18 Da mass differences and corresponded to the addition and dehydration reaction occurrence in C-20 side chain of PPT. Therefore, 24,25-hydrated-PPT, △20(21)- and △20(22)-dehydrated-PPT observed in MS^n were identified as 20(S,R)-Rf_2, Rk_3 and Rh_4, respectively. Malonylated and acetylated ginsenosides with characteristic loss of 86 Da or 42 Da were also

detected. A total of 17 major PPT-type ginsenosides were identified from the extracts of dried and red American ginseng. There were five OCO-type ginsenosides detected in the extracts of American ginseng. According to the specific fragment at *m/z* 491 and saccharide chain composition and position, structural characterizations were obtained. Similarly, another five OLE-type ginsenosides were identified (Table 1).

3.4. Effects of steaming time and temperature on ginsenosides composition in red American ginseng

The holistic chemical profiles of dried and red American ginseng were systematically compared by qualitative and quantitative analysis. The ginsenoside composition differences between dried and red American ginseng, steamed at 100°C or 120°C for 2 h or 4 h or 6 h are shown in Table 2. The effects of steaming time and temperature on the ginsenoside chemical conversion during processing were investigated. As shown in Table 2, the relative peak areas of 59 ginsenosides were calculated by the area ratios of individual peak to total peaks. As the malonyl and acetyl ginsenosides were rather unstable, the relative peak areas of this kind of ginsenosides decreased sharply to undetectable levels with the increasing of steaming time or temperature. Compared to dried American ginseng, the relative peak areas of Rb_1, Rb_2, and so on increased rapidly at 100°C for 2 h, indicating that the malonyl and acetyl ginsenosides degraded to their corresponding neutral ginsenosides. And then Rb_1, Rb_2, Rb_3, Rc, Rd, Rg_1, Re decreased gradually during steaming. After steaming at 120°C for 6 h, Rb_1, Rb_2, Rb_3, Rc, Rd, Rg_1, Re levels were much lower. A number of ginsenoside products increased gradually. Meanwhile, some newly formed ginsenosides among them were identified as 20(R,S)-Rf_2, 20(R)-Rh_1, 20(R)-Rh_2, Rh_3, Rh_4, Rk_1, Rk_2, Rk_3, 20(R)-Rg_2, 20(R)-Rg_3, Rg_4, Rg_5, Rg_6. For OCO- and OLE-type ginsenosides, pseudoginsenoside F_{11} and Ro decreased sharply after steaming for 6 h at 120°C. Correspondingly, newly converted pseudoginsenoside RT_5, Chikusetsusaponin IVa, Zingibroside R_1, and Calenduloside E were identified and relatively quantified.

The results indicated that malonyl and acetyl ginsenosides with high molecular weights are characteristic constituents of dried American ginseng. The neutral and high molecular weight ginsenosides are major components of red American ginseng (100°C), while rare ginsenosides with low molecular weight and less polarity form specific composition of red American ginseng (120°C). Similar results were obtained in ginseng and notoginseng steaming. In our work, the acetyl rare ginsenosides (Rs_3, Rs_4, and Rs_5) were only detected in red American ginseng (100°C and 120°C), which were transformed from Rs_1 and Rs_2. Many studies have revealed that rare ginsenosides in red ginseng enhanced its bioactivities. As discussed above, changes in the PPD, PPT, OCO, OLE types of ginsenosides in red American ginseng were studied systematically, indicated that the steaming time and temperature were significant and influencing parameters of the processing procedure. Due to the chemical complexity in the variation of ginsenosides compositions, multicomponents should be monitored for critically standardizing the conditions and controlling the quality during red American ginseng process. And the multicomponents quantitative assessment could ensure the therapeutic effects of dried and red American ginseng products.

3.5. Summary of steaming-induced ginsenosides conversion of red American ginseng derived from Panax quinquefolium L.

To study the chemical conversion during the process of American ginseng, the ginsenosides markers were identified and relatively quantified. The results demonstrated that the chemical transformation occurred under steaming. The transformation pathways of PPD, PPT, OCO, OLE types of ginsenosides are summarized in Scheme 2, and the content changes of each compound are presented using histograms added beside the corresponding structure. In the Scheme 2, main and secondary transformation pathways are shown with different sized arrows and the specific

Table 2
The relative peak areas of HPLC-MS total ion chromatogram of ginsenosides in dried and red American ginseng steamed at 100°C or 120°C for 2 h or 4 h or 6 h. AG, American ginseng; nd, not detected

Compounds	dried AG	red AG					
		100°C 2 h	100°C 4 h	100°C 6 h	120°C 2 h	120°C 4 h	120°C 6 h
Rb_1	9.49	23.24	22.60	20.45	21.03	9.92	1.04
Rb_2	0.18	1.03	0.88	0.84	0.88	0.22	0.03
Rb_3	1.93	1.60	1.54	1.44	1.47	0.40	0.05
Rc	7.56	5.42	4.53	4.32	4.77	1.07	0.10
Rd	20.17	14.18	12.86	10.51	11.94	7.54	2.14
Gypenoside X VII	2.15	1.76	1.46	1.20	0.69	0.52	0.12
Compound Mc	nd	nd	nd	nd	nd	0.01	0.01
20(S)-Rg_3	0.05	1.98	3.38	4.58	3.63	8.17	9.57
20(R)-Rg_3	nd	1.36	2.25	3.42	2.60	7.19	9.54
F_2	0.24	0.18	0.22	0.12	0.07	0.08	0.07
20(S)-Rh_2	nd	nd	nd	nd	nd	0.01	0.05
20(R)-Rh_2	nd	nd	nd	nd	nd	0.01	0.04
Rk_1	nd	0.62	1.19	1.68	1.31	3.68	4.32
Rg_5	nd	0.67	1.36	1.84	1.44	3.86	4.35
Rk_2	nd	nd	nd	nd	nd	nd	nd
Rh_3	nd	nd	nd	nd	nd	nd	nd
Malonyl-Rb_1	12.40	2.85	nd	nd	nd	nd	nd
Malonyl-Rb_2	0.56	0.06	nd	nd	nd	nd	nd
Malonyl-Rb_3	0.69	0.03	nd	nd	nd	nd	nd
Malonyl-Rc	1.38	0.23	nd	nd	nd	nd	nd
Malonyl-Rd	9.68	1.20	nd	nd	nd	nd	nd
Quinquefolium R_1	6.92	5.83	5.62	4.90	4.40	2.63	0.25
Pseudo-F_8	0.57	0.08	0.07	0.06	0.06	0.04	0.02
Rs_1	0.13	0.09	0.08	0.07	0.08	0.03	0.01
Rs_2	0.29	0.12	0.11	0.10	0.11	0.04	0.01
Pseudo-RC_1	8.53	2.38	2.03	1.43	2.07	1.46	0.51
Quinquefolium III	2.94	0.33	0.29	0.21	0.24	0.21	0.12
20(S)-Rs_3	nd	2.59	1.49	0.41	0.35	0.27	0.15
20(R)-Rs_3	nd	0.08	0.14	0.26	0.20	1.04	2.00
Rs_4	nd	0.01	0.05	0.07	0.06	0.29	0.50
Rs_5	nd	0.01	0.06	0.08	0.08	0.39	0.69
Quinquefolium I	0.54	0.39	0.37	0.33	0.36	0.24	0.09
Re	31.92	16.57	16.03	14.72	14.04	3.31	0.14
Rg_1	1.63	1.18	0.65	0.53	0.65	0.23	0.21
20(S)-Rg_2	2.47	2.04	4.09	4.80	3.25	9.30	10.81
20(R)-Rg_2	nd	1.13	2.55	3.24	2.07	8.08	11.51
F_1	nd	0.00	0.01	0.01	0.01	0.02	0.03
20(S)-Rf_2	nd	0.00	0.02	0.04	0.02	0.35	1.02
20(R)-Rf_2	nd	0.00	0.01	0.03	0.01	0.31	1.43
Rg_6	nd	0.79	1.83	2.08	1.43	5.71	8.37
Rg_4	0.04	1.09	2.47	2.76	1.91	6.88	10.08
20(S)-Rh_1	0.01	0.05	0.15	0.17	0.24	0.46	1.09
20(R)-Rh_1	nd	0.03	0.09	0.11	0.16	0.42	1.38
Rk_3	nd	0.02	0.04	0.05	0.08	0.21	0.72
Rh_4	nd	0.02	0.06	0.07	0.11	0.30	0.99
Malonyl-Rg_1	2.06	nd	nd	nd	nd	nd	nd
Acetyl-Rg_1	1.24	0.01	nd	nd	nd	nd	nd
20(S)-acetyl-Rg_2	0.05	0.01	0.02	0.02	0.02	0.06	0.20
20(R)-acetyl-Rg_2	nd	nd	nd	nd	nd	0.05	0.17
Ro	14.57	7.92	4.59	3.85	6.23	5.89	2.82
Pseudo-RT_1	1.92	0.92	0.80	0.64	1.00	0.79	0.11
Chikusetsusaponin IVa	2.00	2.09	1.76	1.31	1.60	2.62	2.93
Zingibroside R_1	0.84	0.38	0.22	0.29	0.20	1.01	0.82
Calenduloside E	0.10	0.13	0.22	0.31	0.21	0.28	0.40
24(S)-Pseudo-F_{11}	0.68	0.28	0.26	0.20	0.25	0.20	0.18
24(R)-Pseudo-F_{11}	12.29	4.08	5.80	2.75	3.87	5.39	4.68
Pseudo-RT_2	3.46	1.94	1.25	0.78	1.63	1.44	0.02
Pseudo-RT_5	nd	0.01	0.02	0.04	0.05	0.10	0.57
24(R)-Vina-R_1	0.21	0.16	0.09	0.05	0.08	0.02	0.01

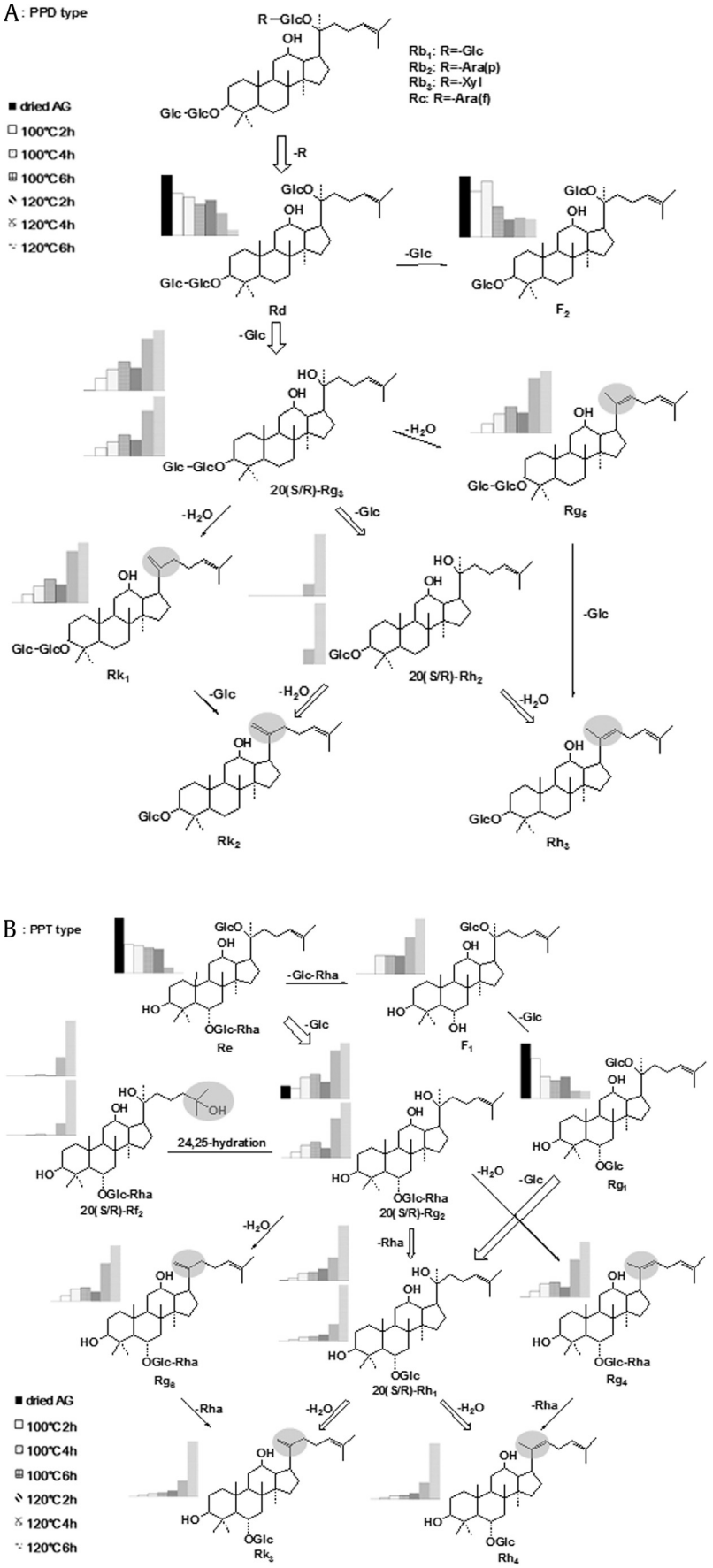

Scheme 2. Scheme 2. The transformation pathways of four types of ginsenosides. (A) protopanaxadiol; (B) protopanaxatriol; (C) ocotillol; (D) oleanane. OCO, ocotillol; OLE, oleanane; PPD, protopanaxadiol; PPT, protopanaxatriol.

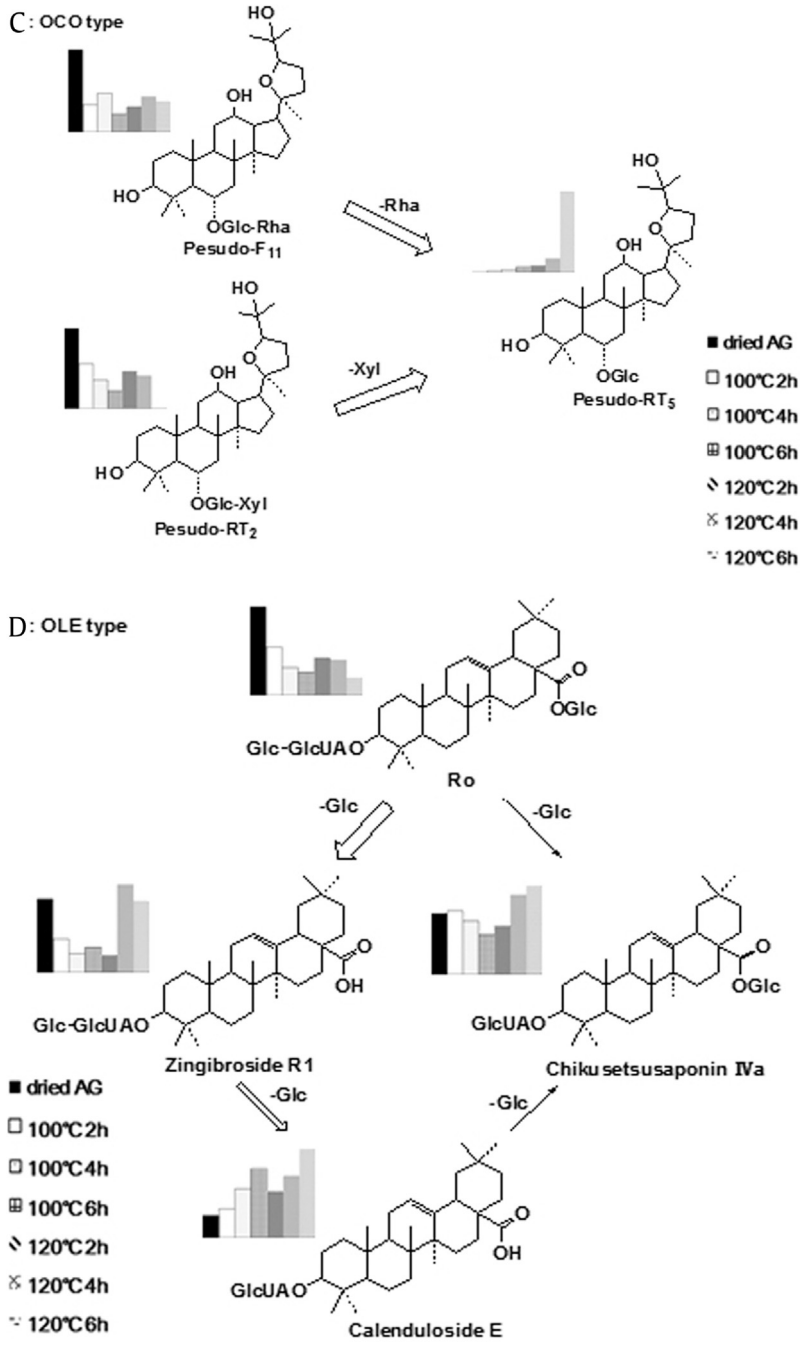

Scheme 2. (*continued*).

structure product ginsenosides are highlighted with gray background. The characteristic transformation mechanisms detected were discussed.

Ginsenosides Rb_1, Rb_2, Rb_3, Rc as original PPD ginsenosides transformed to Rd by the hydrolysis of glycosylation moiety at C-20 terminus, leading the relative peak areas declined. Rd could be hydrolyzed to 20(S)-Rg_3 with its epimer 20(R)-Rg_3 and its isomer F_2 by the loss of glucose residue at C-20 and C-3, respectively. Furthermore, 20(S,R)-Rg_3 produced 20(S,R)-Rh_2 through the hydrolysis of glycosylation moiety at C-3 terminus. The 20(21) and △20(22) isomers Rk_1 and Rg_5 were generated from 20(S,R)-Rg_3 through dehydration at C-20. And then, 20(S,R)-Rh_2, Rk_1 and Rg_5 could convert to 20(21) and △20(22) isomers Rk_2 and Rh_3. The results demonstrated that the transformation pathways of PPT ginsenosides were similar to those of PPD ginsenosides, as the characteristic conversion shown in Scheme 2(A) and 2(B). The products were observed involving the glycosylation moiety hydrolysis at C-20 terminus to form 20(S,R)-Rg_2 and at C-6 to form 20(S,R)-Rh_1 and 20(21) or △20(22) dehydration at C-20 to yield Rg_6 and Rg_4. There is also a specific transformation of PPT ginsenosides, C24 and C-25 hydration, and gave rise to 20(S,R)-Rf_2. In the published reports, the transformation mechanisms and pathways of PPD and PPT ginsenosides were described during fresh ginseng steaming [8,9,11,27]. And the previous results partially agreed with our findings obtained from American ginseng steaming in related transformation mechanisms. Because

of the differences in ginsenoside compositions of ginseng and American ginseng, the transformation pathways were not identical.

For OCO- and OLE-type ginsenosides, the losses of glycosylated substitution were the main chemical transformation pathways. The possible ginsenoside products were deduced and shown in Scheme 2(C) and 2(D). With regard to OCO- and OLE-type ginsenosides, the chemical transformations have not been systematically studied in American ginseng research to our knowledge.

The malonyl and acetyl ginsenosides released malonic and acetic acid by demalonylation and deacetylation reactions, respectively, to yield their corresponding neutral ginsenosides. Malonyl and acetyl ginsenosides could reportedly convert to neutral ginsenosides and provide the acidic environment to further promote degradation of neutral ginsenosides [10,11]. Under steaming, acetyl ginsenosides produced their corresponding neutral ginsenosides firstly and subsequently transformed to their corresponding rare ginsenosides with low molecular weight. In our study, the acetyl rare ginsenosides were detected in red American ginseng for the first time, transformed from their corresponding acetyl ginsenosides by hydrolysis of terminus glucosylation moiety and dehydration at C-20. This result demonstrated that acetyl ginsenosides presented two kinds of transformation pathways, which have not been reported yet.

Our results provide related chemical transformation of four types of ginsenosides during American ginseng processing. These ginsenosides generated in steaming of American ginseng may be helpful for evaluating pharmacological effects and bioactive constituents' definition.

4. Conclusions

In summary, the HPLC-MS^n-based multicomponent profiling was developed to assess the holistic qualities of dried and red American ginseng. The specific fragments of four major types of ginsenosides were PPD at *m/z* 459, PPT at *m/z* 475, OCO at *m/z* 491, and OLE at *m/z* 455. And the aglycone of chemically-derived ginsenosides produced specific fragments at *m/z* 441 and *m/z* 457 for △20(21)- or △20(22)-dehydrated PPD and △20(21)- or △20(22)-dehydrated PPT, meanwhile *m/z* 493 for 24,25-hydrated PPT were also observed in MS^n. Based on the characteristic fragmentation pathways of four types ginsenosides, the structure of 59 multiginsenoside components in dried and red American ginseng were analyzed. The chemical markers that could discriminate dried and red American ginsengs were discussed, and the possible transformation mechanisms were summarized. The ginsenosides composition of red American ginseng changed with the increase in the steaming time and temperature. The ginsenosides with higher molecular weight and more polarity converted to the rare ones with lower molecular and less polarity via hydrolysis of saccharides substituents. The malonyl or acetyl ginsenosides transformed to their corresponding neutral ginsenosides and acetyl rare ginsenosides. And the production of 20(R)-ginsenosides epimers, dehydrated, and hydrated ginsenosides were the specific constituents of red American ginseng. The results, discussed above, are definitely helpful for quality assessment and standardizing the processing procedures of red American ginseng. Furthermore, the results also provided a scientific basis for the research on biological compositions, which is responsible for the pharmacological efficacy of red American ginseng and the safe usage of American ginseng in clinic.

Conflicts of interest

The authors declare that they have no competing interests.

Acknowledgments

This work was supported by the Science and Technology Development Plan Project of Jilin Province (20160520181JH, 20170414027GH), the "13th Five-Year" Science and Technology Research Project of Jilin Province Education Department (2016 No. 30), the Special Scientific Research Fund of Agricultural Public Welfare Profession of China (20130311106) and the Training Plan of Hundreds of Outstanding Treachers of Changchun University of Chinese Medicine (No. 2017086).

References

[1] Yuan CS, Wang CZ, Wicks SM, Qi LW. Chemical and pharmacological studies of saponins with a focus on American ginseng. J Ginseng Res 2010;34:160–7.
[2] Kim DH. Chemical diversity of panax ginseng panax quinquifolium, and panax notoginseng. J Ginseng Res 2012;36:1–15.
[3] Qi LW, Wang CZ, Yuan CS. Isolation and analysis of ginseng: advances and challenges. Nat Prod Rep 2011;28:467–95.
[4] Qi LW, Wang CZ, Yuan CS. Ginsenosides from American ginseng: chemical and pharmacological diversity. Phytochemistry 2011;72:689–99.
[5] Ko SK, Cho OS, Bae HM, Sohn UD, Im BO, Cho SH, Chung SH, Lee BY. Change of ginsenoside composition of various American ginseng roots. J Korean Soc Appl Biol Chem 2009;52:198–201.
[6] Kim WY, Kim JM, Han SB, Lee SK, Kim ND, Park MK, Kim CK, Park JH. Steaming of ginseng at high temperature enhances biological activity. J Nat Prod 2000;63:1702–4.
[7] Nam KY. The comparative understanding between red ginseng and white ginseng, processed ginsengs (Panax ginseng C. A. Meyer). J Ginseng Res 2005;29:1–18.
[8] Xie YY, Luo D, Cheng YJ, Ma JF, Wang YM, Liang QL, Luo GA. Steaming-induced chemical transformations and holistic quality assessment of red ginseng derived from Panax ginseng by means of HPLC-ESI-MS/MS^n-based multicomponent quantification fingerprint. J Agric Food Chem 2012;60:8213–24.
[9] Wu W, Qin QJ, Guo YY, Sun JH, Liu SY. Studies on the chemical transformation of 20(S)-PPT-type ginsenosides Re, Rg_2, and Rf by using RRLC-Q-TOF-MS. J Agric Food Chem 2012;60:10007–14.
[10] Kim MH, Lee YC, Choi SY, Cho CW, Rho J, Lee KW. The changes of ginsenoside patterns in red ginseng processed by organic acid impregnation pretreatment. J Ginseng Res 2011;35:497–503.
[11] Liu Z, Xia J, Wang CZ, Zhang JQ, Ruan CC, Sun GZ, Yuan CS. Remarkable impact of acidic ginsenosides and organic acids on ginsenoside transformation from fresh ginseng to red ginseng. J Agric Food Chem 2016;64:5389–99.
[12] Lee MR, Yun BS, Sung CK. Comparative study of white and steamed black Panax ginseng, P. quinquefolium, and P. notoginseng on cholinesterase inhibitory and antioxidative activity. J Ginseng Res 2012;36:93–101.
[13] Ren GX, Chen F. Degradation of ginsenosides in American ginseng (Panax quinquefolium) extracts during microwave and conventional heating. J Agric Food Chem 1999;47:1501–5.
[14] Sun BS, Xu MY, Li Z, Wang YB, Sung CK. UPLC-Q-TOF-MS/MS analysis for steaming times-dependent profiling of steamed panax quinquefolius and its ginsenosides transformations induced by repetitious steaming. J Ginseng Res 2012;36:277–90.
[15] Zeng F, Wang XM, Yang M, Lu ZQ, Guo DA. Fingerprint analysis of different Panax herbal species by HPLC-UV method. J Chin Pharm Sci 2007;16:277–81.
[16] Zhang X, Ma X, Si B, Zhao Y. Simultaneous determination of five active hydrolysis ingredients from *Panax quinquefolium* L. by HPLC-ELSD. Biomed Chromatogr 2011;25:646–51.
[17] Wang J, Bai HL, Liu CM, Li L. Isolation and purification of ginsenosides from plant extract of *Panax quinquefolium* L. by high performance centrifugal partition chromatography coupled with ELSD. Chromatographia 2009;71:267–71.
[18] Sun XB, Chen P, Cook SL, Jackson GP, Harnly JM, Harrington PB. Classification of cultivation locations of *Panax quinquefolius* L. samples using high performance liquid chromatography–electrospray ionization mass spectrometry and chemometric analysis. Anal Chem 2012;84:3628–34.
[19] Steinmann D, Ganzera M. Recent advances on HPLC/MS in medicinal plant analysis. J Pharm Biomed Anal 2011;55:744–57.
[20] Li M, Hou XF, Zhang J, Wang SC, Fu Q, He LC. Applications of HPLC/MS in the analysis of traditional Chinese medicines. J Pharm Anal 2011;1:81–91.
[21] Yang M, Sun J, Lu Z, Chen G, Guan S, Liu X, Jiang B, Ye M, Guo DA. Phytochemical analysis of traditional Chinese medicine using liquid chromatography coupled with mass spectrometry. J Chromatogr A 2009;1216:2045–62.
[22] Shi Y, Sun CJ, Zheng B, Gao B, Sun AM. Simultaneous determination of ten ginsenosides in American ginseng functional foods and ginseng raw plant materials by liquid chromatography tandem mass spectrometry. Food Anal Methods 2013;6:112–22.
[23] Yang WZ, Ye M, Qiao X, Liu CF, Miao WJ, Bo T, Tao HY, Guo DA. A strategy for efficient discovery of new natural compounds by integrating orthogonal column chromatography and liquid chromatography/mass spectrometry analysis: its application in Panax ginseng, Panax quinquefolium and Panax

notoginseng to characterize 437 potential new ginsenosides. Anal Chim Acta 2012;739:56–66.
[24] Qi LW, Wang HY, Zhang H, Wang CZ, Li P, Yuan CS. Diagnostic ion filtering to characterize ginseng saponins by rapid liquid chromatography with time-of-flight mass spectrometry. J Chromatogr A 2012;1230:93–9.
[25] Wan JY, Liu P, Wang HY, Qi LW, Wang CZ, Li P, Yuan CS. Biotransformation and metabolic profile of American ginseng saponins with human intestinal microflora by liquid chromatography quadrupole time-of-flight mass spectrometry. J Chromatogr A 2013;1286:83–92.
[26] Park HW, In G, Kim JH, Cho BG, Han GH, Chang IM. Metabolomic approach for discrimination of processed ginseng genus (Panax ginseng and Panax quinquefolius) using UPLC-QTOF MS. J Ginseng Res 2014;38:59–65.
[27] Wu W, Sun L, Zhang Z, Guo YY, Liu SY. Profiling and multivariate statistical analysis of Panax ginseng based on ultra-high-performance liquid chromatography coupled with quadrupole-time-of-flight mass spectrometry. J Pharm Biomed Anal 2015;107:141–50.
[28] Domon B, Costello CE. A systematic nomenclature for carbohydrate fragmentations in FAB-MS/MS spectra of glycoconjugates. Glycoconj J 1988;5:397–409.
[29] Liu S, Cui M, Liu Z, Song F. Structural analysis of saponins from medicinal herbs using electrospray ionization tandem mass spectrometry. J Am Soc Mass Spectrom 2004;15:133–41.